Mathematical Biosciences and Engineering

MBE, 19(1): 972–996.
DOI: 10.3934/mbe.2022045
Received: 14 September 2021
Accepted: 15 November 2021
Published: 23 November 2021

http://www.aimspress.com/journal/MBE

Research article

EWM-based design method for distortional buckling of cold-formed thin-walled lipped channel sections with holes

Xingyou Yao*

School of Civil Engineering and architecture, Nanchang Institute of Technology, Nanchang, 330000, China

* **Correspondence:** Email: yaoxingyoujd@163.com; Tel: +8615079190103.

Abstract: The distortional buckling is easy to occur for the cold-formed steel (CFS) lipped channel sections with holes. There is no design provision about effective width method (EWM) to predict the distortional buckling strength of CFS lipped channel sections with holes in China. His aim of this paper is to present an proposal of effective width method for the distortional buckling strength of CFS lipped channel sections with holes based on theoretical and numerical analysis on the partially stiffened element and CFS lipped channel section with holes. Firstly, the prediction methods for the distortional buckling stress and distortional buckling coefficients of CFS lipped channel sections with holes were developed based on the energy method and simplified rotation restrained stiffness. The accuracy of the proposed method for distortional buckling stress was verified by using the finite element method. Then the modified EWM was proposed to calculate the distortional buckling strength and the capacity of the interaction buckling of CFS lipped channel sections with holes based on the proposal of distortional buckling coefficient. Finally, comparisons on ultimate capacities of CFS lipped channel sections with holes of the calculated results by using the modified effective width method with 347 experimental results and 1598 numerical results indicated that the proposed EWM is reasonable and has a high accuracy and reliability for predicting the ultimate capacities of CFS lipped channel section with holes. Meanwhile, the predictions by the North America specification are slightly unconservative.

Keywords: cold-formed steel; holes; partially stiffened element; distortional buckling; ultimate strength; effective width method

1. Introduction

Cold-formed steel lipped channel sections have been widely used in steel building constructions as columns in wall and beams in floor or roof. The web, flange, and lip of lipped channel section are usually defined as the stiffened element, partially stiffened element, and unstiffened element as shown in Figure 1. The lipped channel section may fail in local buckling, distortional buckling, and overall buckling or interaction buckling of these buckling modes. The local buckling displays the deformation of plate. The distortional bucking mode means a rotational deformation of the partially stiffened element about the flange-web junction. The overall buckling means the flexual, tortional, or flexural-tortional deformation of the whole section. However, in order to install the electrical, plumbing, and heating pipes, the circular or rectangular holes are observed in the web of CFS lipped channel sections. The presences of these holes cause the decrease of rotation restraint stiffness of the web to the flanges and make the distortional buckling easy to occur.

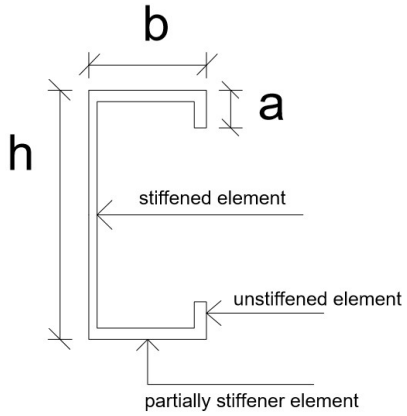

Figure 1. Definitions of lipped channel section.

The distortional buckling would control the capacities of CFS lipped channel sections because of the large width-to-thickness ratio of the partially stiffener element and application of high strength steel. Lau and Hancock [1] firstly studied the distortional buckling mode of CFS sections and developed a closed-form solution of distortional buckling stress. Then many theoretical, numerical, and experimental studies have been carried out on the distortional buckling [2–7] and the design methods of elastic buckling stress and ultimate strength for the distortional buckling of CFS lipped channel sections without holes were included some main design specification about CFS members.

The experimental and numerical studies on the buckling behavior and design method of CFS lipped channel sections with holes were carried out by some researchers. The buckling behavior and design method for CFS axial compression columns with circular holes were conducted by Ortiz-Colberg [8], Sivakumaran [9], and He and Zhao [10], but the design method of distortional buckling was not considered in these researches. The distortional buckling and interaction buckling were observed in the tests for CFS lipped channel sections with slotted holes under axial compression [11,12]. The tests showed that the presence of the slotted holes caused a slight decrease in the ultimate capacity and changed the length of the distortional buckling half wavelength. The

effect of rectangular hole on the buckling behavior and ultimate capacity of CFS lipped channel column subjected to axial compression was also studied by Miller et al. [13], Abdel-Rahman [14], Pu et al. [15], Hu et al. [16], Guo et al. [17], Guo et al. [18] and Yao [19]. The test results demonstrated that the rectangular hole led the change of bucking mode of some specimens and decreased the ultimate strength. Meanwhile, the rectangular hole made CFS lipped channel sections prone to display distortional buckling. Zhao et al. [20] and Moen et al. [21] conducted the experiments of CFS lipped channel beam with rectangular holes and plain channel beam with rectangular holes. The CFS beam with holes displayed the distortional buckling and the interaction buckling. The presence of rectangular hole resulted in the decrease of the ultimate capacity and the modified direct strength method was presented.

In order to develop the design method of the distortional buckling based on effective width method and direct strength method for CFS lipped channel sections with holes, the calculated methods of the distortional buckling coefficient or the distortional buckling capacity for the lipped channel section with holes have been presented by some researchers. Zhou and Yu [22] presented the equivalent modulus method to calculate the distortional buckling stress of CFS axial compression member with holes. The simplified methods of the distortional buckling loads of CFS lipped channel column and beam with holes were developed based on theoretical and finite element analysis [23]. The modified formula of the distortional buckling coefficient for axial compression member with circular holes was proposed by Yao et al. [24] based on numerical analysis. Based on experiments and theoretical analysis, the modifications to the direct strength method were presented by Moen and Schafer [25] and Yao and Rasmussen [26] so that it can be used to calculate the distortional buckling strength of CFS lipped channel section with holes under axial compression.

The American Iron and Steel Institute (AISI) [27] adopts the effective width method and direct strength method to predict the distortional buckling strength of CFS channel section with holes. However, the reduced effective width method is only suitable to the member with the ratio of diameter to height of web being less than 0.5. The elastic buckling capacity of member with holes used in direct strength method needs to be calculated by using finite element method or complicated formula. Meanwhile, there is no relevant provision to calculate distortional buckling capacity of CFS lipped channel section with holes in the Chinese cold-formed steel specification [28].

Recently, some significant work has been reported on the strength of CFS channel section with holes covering the web crippling by Uzzaman et al. [29,30] and Lian et al. [31−34] and the shear capacity by Pham [35] and Keerthan et al. [36]. Meanwhile, the experimental and numerical studies on CFS channel section with edge-stiffened holes have reported for the axial strength of single channel [37] and back-to-back channel [38]. The studied results showed that the ultimate capacity of channel with edge-stiffened holes was greater than that of channel with plain hole. Meanwhile, some other work has been conducted on the channel section with edge-stiffened hole covering the web crippling by Uzzaman et al. [39,40] and the moment capacity by Chen et al. [41].

As mentioned previously literatures, limited work has been reported on design method for the distortional buckling of CFS lipped channel section with holes in the web based on effective width method. The aim of this paper is to present a novel effective width method to calculate the distortional strength and ultimate capacity of CFS lipped channel section with holes. The design formula of elastic distortional buckling stress for CFS lipped channel section with holes is developed firstly. The quality and reliability of the design formula is validated by using finite element results. Then the EWM-based desgin method is given based on the proposed method of the distortional buckling coefficient. Finally, the

comparisons on the ultimate strength for CFS lipped channel column and beam with holes of predictions obtained from the proposed effective width method with test results and finite element results are carried out.

2. Elastic distortional buckling of cold-formed steel lipped channel section with holes

2.1. Calculation of the distortional buckling stress

The distortional buckling analytical model of CFS lipped channel section with hole is shown in Figure 2, where b and a are the width of the flange and the width of the lip, respectively, σ is the axial compression stress, θ is the rotation angle of the distortional buckling deformation, k_θ is the rotation restrained stiffness of the web with hole. The basic assumptions are that the lip is an elastic bearing beam and has no restrain stiffness for the flange (partially stiffened element) and the shear stress around the flange and the transverse stresses of the two longitudinal edges are equal to zero.

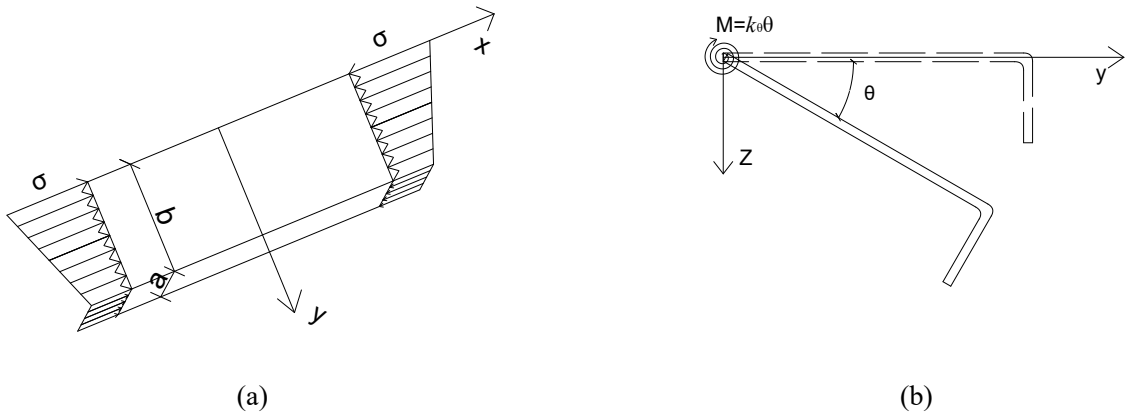

(a) (b)

Figure 2. Distortional buckling analytical model. (a) Coordinated system of the partially stiffened element. (b) Deformation of distortional buckling for the partially stiffened element.

The differential equation of the partially stiffened element is shown as Eq (1):

$$\frac{\partial^4 w}{\partial x^4} + 2\frac{\partial^4 w}{\partial x^2 \partial y^2} + \frac{\partial^4 w}{\partial y^4} = \frac{\sigma_x t}{D}\frac{\partial^2 w}{\partial x^2} \tag{1}$$

where D, E, t, and w are the flexural rigidity of unit plate, the elastic modulus of steel, the thickness of plate, and the deformation of the partially stiffened element, respectively.

The deflected shape function for the partially stiffened element is shown as follow:

$$w = By\cos\left(\pi x / L\right) \tag{2}$$

where B is the coefficient, L is the length of the partially stiffened element. The Eq (2) satisfies the geometric boundary conditions as follows: when $x = 0$ or $x = \mathrm{L}$ and $y = 0$, $w = 0$; when $y = b$, $w \neq 0$.

When the maximum compression stress acts at the stiffened edge (y = 0), the bending strain energy of the flange U_{flange}, the bending strain energy of the lip V_{lip}, the rotational restraint strain energy of the web with hole U_{web}, the potential energy of the flange V_{flange}, and the potential energy of the lip V_{lip} can be obtained as follows:

The bending strain energy of the flange is

$$U_{flange}=\frac{1}{2}D\int_{-L/2}^{L/2}\int_{0}^{b}\left\{\left(\frac{\partial^2 w}{\partial x^2}+\frac{\partial^2 w}{\partial y^2}\right)^2-2(1-\upsilon)\left[\frac{\partial^2 w}{\partial x^2}\times\frac{\partial^2 w}{\partial y^2}-\left(\frac{\partial^2 w}{\partial x\partial y}\right)^2\right]\right\}dydx=\frac{1}{4}B^2DbL\left(\frac{\pi}{L}\right)^2\left[\left(\frac{\pi}{L}\right)^2 b^2/3+2(1-\nu)\right] \tag{3}$$

The bending strain energy of the lip is

$$U_{lip}=\frac{1}{2}EI\int_{-L/2}^{L/2}\left(\frac{\partial^2 w}{\partial x^2}\right)^2_{y=b}dx=\frac{1}{4}B^2EI\left(\frac{\pi}{L}\right)^4 b^2L \tag{4}$$

The rotational restraint strain energy of the web is

$$U_{web}=\frac{1}{2}k_{\theta hole}\int_{-L/2}^{L/2}\left(\frac{\partial w}{\partial x}\right)^2_{y=0}dx=\frac{1}{4}B^2k_{\theta hole}L \tag{5}$$

The potential energy of the flange is

$$V_{flange}=-\frac{1}{2}\int_{-L/2}^{L/2}\int_{0}^{b}\sigma_x\left(\frac{\partial w}{\partial x}\right)^2 tdydx=-\frac{1}{2}\int_{-L/2}^{L/2}\int_{0}^{b}\sigma_{web}(1-(1-\alpha)y/b)\left(\frac{\partial w}{\partial x}\right)^2 tdydx=-\frac{1}{4}B^2b^3tL\left(\frac{\pi}{L}\right)^2(1/12+\alpha/4)\sigma_{web} \tag{6}$$

The potential energy of the lip is

$$V_{lip}=-\frac{1}{2}at\int_{-L/2}^{L/2}\sigma_{lip}\left(\frac{\partial w}{\partial x}\right)^2_{y=b}dx=-\frac{1}{2}at\int_{-L/2}^{L/2}\sigma_{web}\alpha\left(\frac{\partial w}{\partial x}\right)^2_{y=b}dx=-\frac{1}{4}B^2atb^2L\left(\frac{\pi}{L}\right)^2\alpha\sigma_{web} \tag{7}$$

where σ_{web} is the compression stress of the stiffened edge, $k_{\theta\text{hole}}$ is the rotational restraint stiffness of the web with hole, α is the factor of non-uniform stress distribution of the flange, $\alpha=\sigma_{\min}/\sigma_{\max}$, ν is the poisson's ratio.

The total elastic buckling potential energy of the partially stiffened element is calculated as Eq (8).

$$\prod=U_{flange}+U_{web}+U_{lip}+V_{lip}+V_{flange} \tag{8}$$

Substituting Eqs (3)−(7) in Eq (8) and assuming $\partial\prod/\partial B=0$, the distortional buckling stress can be obtained as Eq (9).

$$\sigma_{crd.web}=\frac{k_{\theta hole}/(\pi/L)^2+Db((\pi b/L)^2/3+2(1-\upsilon))+EI(\pi b/L)^2}{tb^3(1/12+\alpha/4)+atb^2\alpha} \tag{9}$$

when we assign $\partial\sigma_{crd.web}/\partial L=0$, the half wavelength of the distortional buckling can be calculated by using Eq (10).

$$L_{crd}=\pi\sqrt[4]{\left(b^3D/3+EIb^2\right)/k_{\theta hole}} \tag{10}$$

When the maximum compression stress acts at the unstiffened edge (lip), the stress and the half wavelength of the distortional buckling can be obtained as follows by using the same method as the maximum compression stress acting at the stiffened edge.

$$\sigma_{crd.lip} = \frac{k_{\theta hole} / (\pi / L)^2 + Db((\pi b / L)^2 / 3 + 2(1-\upsilon)) + EI(\pi b / L)^2}{tb^3(1/4 + \alpha/12) + atb^2} \tag{11}$$

$$L_{crd} = \pi \sqrt[4]{\left(b^3 D / 3 + EIb^2\right) / k_{\theta hole}} \tag{12}$$

The rotational restraint stiffness of web with hole should be calculated firstly if the stress and the half wavelength of the distortional buckling are calculated by using Eqs (9)−(12).

2.2. Web rotational restraint stiffness

An elastic finite element model was developed by using ABAQUS program to study the influence of a hole on the rotational restraint stiffness of CFS lipped channel section. The web with a rectangular hole was performed as a simply-supported plate with the length of 540 mm which is equal to a distortional buckling half wavelength as shown in Figure 3. The width and the thickness of plate are 90 mm and 2 mm. The length of the rectangular hole is 150 mm and the heights of the rectangular hole are 30, 40 and 50 mm. The ideal elastoplastic model was used in FEM. The mesh size is 5 mm × 5 mm. The rotations with the magnitudes varying as a sine half wave are loaded at two longitudinal edges. Each node at two longitudinal edges is performed a rotation and the associated moment which means the rotational restraint stiffness per unit length can be obtained from ABAQUS and depicted in Figure 4. As shown in Figure 4, the presence of the rectangular hole results in a sharp reduction of rotational restraint stiffness at the zone of the hole and has no distinct influence on the rotational restraint stiffness away from the rectangular hole. The ratio of height of the hole to the width of plate has no distinct effect on the rotation restraint stiffness except for peaks of stiffness at the edges of hole. The rotational restraint stiffness of the zone of the hole can be ignored because it approaches zero. Therefore, if k_θ expresses the total of the transverse rotational restrain stiffness of the plate without the hole, the reduced rotational restrain stiffness $k_{\theta hole}$ considering the effect of the hole can be calculated by using Eq (13) approximately.

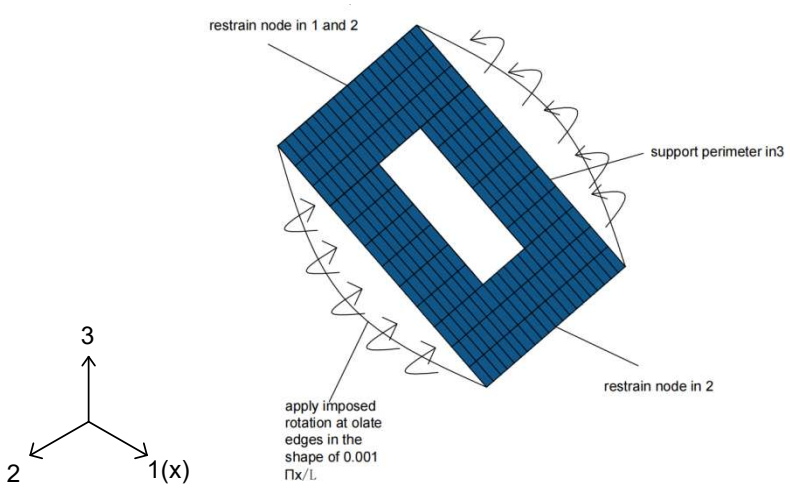

Figure 3. Finite element model of a simply-supported plate with rectangular hole.

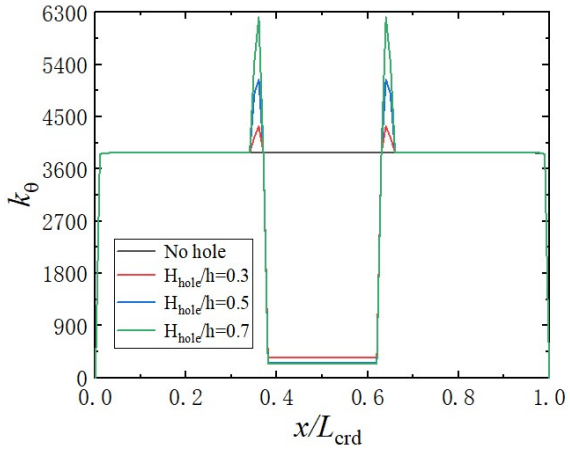

Figure 4. Comparison on the rotation restrain stiffness of plate with hole.

$$k_{\theta hole} = \left(1 - \frac{L_{hole}}{L_{crd}}\right) k_\theta \tag{13}$$

where, L_{hole} and L_{crd} are the length of the hole and the distortional buckling half wavelength of CFS lipped channel section.

Yao [7] indicated that the value of k_θ equals approximately a constant of $2D/h$ and $4D/h$ for axial compression member and bending member when CFS lipped channel member without hole fails in distortional buckling. Meanwhile, the value of k_θ can be determined as $(2+\alpha_w)D/h$ for CFS lipped channel section with varying stress in the web, where α_w is the factor of non-uniform stress distribution of the web. Then the distortional buckling half wavelength of CFS lipped channel section with hole can be obtained as Eq (14) resulted from Eqs (12) and (13).

$$L_{crd.hole} = \pi \sqrt[4]{\frac{b^2 h}{6(1+0.5\alpha_w)\left(1 - \frac{L_{hole}}{L_{crd}}\right)}\left(b + 3EI/D\right)} \tag{14}$$

2.3. Verification for elastic distortional buckling stress

The finite element program ABAQUS [29] was used to analysis the distortional buckling stress and the ultimate strength of CFS lipped channel section with holes in order to verify the accuracy of the proposed method. The S4R shell element was selected for modeling the axial compression member with holes and bending member with holes. The ideal elastoplastic model was used in FEM. The mesh size is 5 mm × 5 mm as shown in Figure 5. The ends of the axial compression member with holes were fixed as shown in Figure 5(a), by constraining five degrees of freedom of the reference point RP1 at the loading end (2 translation degrees of freedom and 3 rotational degree of freedom, releasing U1 degrees of freedom to apply the load) and six degrees of freedom of the reference point RP2 were constrained at the other end. In order to obtain the distortional buckling stress, the interaction line of the web and the flange was constrained in direction 3. The constraint condition of the bending member with holes was shown in Figure 5(b). Two ends were constrained in direction 2−4 and the moments were applied at two ends. The mid-section of bending member was constrained in direction 1. In order to obtain the distortional buckling stress of bending member with

holes, the interaction line of the web and the flange was constrained in direction 3. The eigenvalue buckling analysis was performed to find the elastic distortional buckling stress of CFS lipped channel section with holes. Two phases need to conduct in order to obtain the ultimate strength of CFS channel section with holes. Firstly, an eigenvalue buckling analysis was performed to find the first elastic buckling mode of the member with holes. The $L/1000$ magnitude of the initial geometric imperfection was applied to the first eigen-mode to produce the geometric imperfection of FEM. Secondly, nonlinear analysis considering both material and geometric nonlinear was carried out by using the arc-length method to get the ultimate capacity.

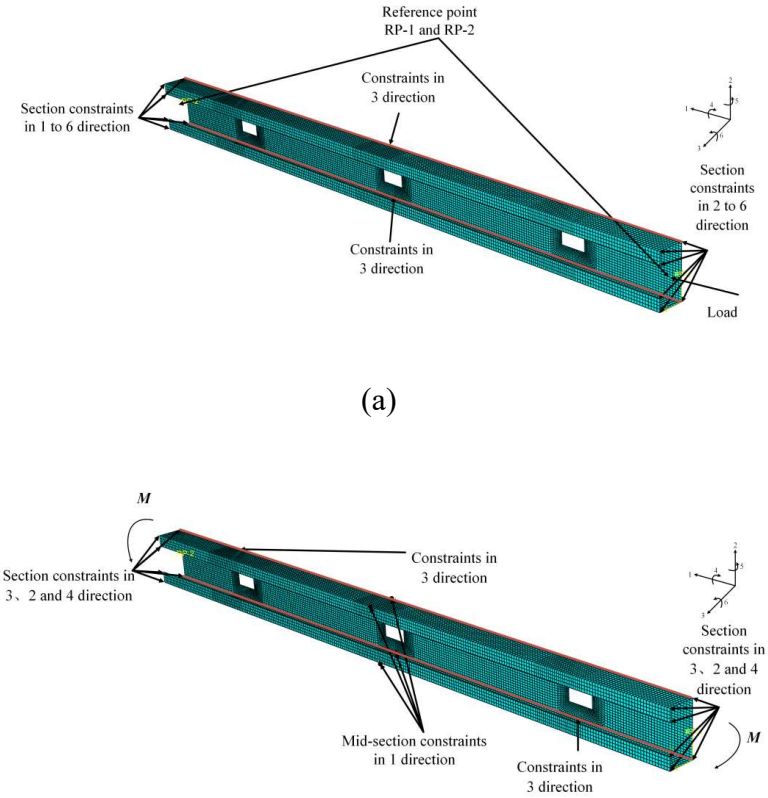

Figure 5. Finite element model of CFS lipped channel section with holes. (a) Axial compression members with holes. (b) Bending members with holes.

The selected sectional dimensions are that the width of the flange is 90mm, the thickness of the plate is 2 mm, the lip-to-flange width ratio is 0.05, 0.1, 0.15, 0.2, 0.25, 0.3, 0.35 and 0.4, the web-to-flange width ratio is 1, 2, and 3 for axial compression member and 3, 4 and 5 for bending member. The ratio of height of the rectangular hole to the width of the web is 0.5, the length-to-height ratio of the rectangular hole is 1, 2, 3 and 4. The ratio of the diameter of circular hole to the width of the web is 0.3, 0.5 and 0.7. The comparisons on distortional buckling stress between calculated results using the proposed formulas and finite element results are shown in Tables 1−4 for axial compression member with rectangular hole, axial compression member with circular hole, bending member with rectangular hole, bending member with rectangular hole, respectively. Where f_{crd} and $f_{crd.A}$ are the distortional buckling stress predicted by using the proposed formulas and finite element result, respectively. The statistical results of comparisons on distortional

buckling stress of predicted results with finite element results for all selected members are listed in Table 5. The mean value is 0.9899 with the corresponding coefficient of variation of 0.0524. The comparison as shown in Tables 1−5 indicated a great agreement and accuracy for the distortional buckling stress of CFS lipped channel sections with holes by using the proposed Eqs (9) and (11).

Table 1. Comparison on distortional buckling stress between the proposed method and the finite element method for axial compression member with rectangular hole.

	h	H_{hole}	L_{hole}	a = 4.5	a = 9	a = 13.5	a = 18	a = 22.5	A = 27	a = 31.5	a = 36
f_{crd}	90	45	45	103.17	178.87	263.36	346.98	424.71	495.14	556.76	616.26
			90	96.77	169.12	251.37	334.75	411.66	479.74	535.67	592.78
			135	89.64	158.63	238.7	322.02	398.15	463.81	513.68	568.31
			180	81.46	147.21	225.22	308.73	384.14	447.29	490.66	542.69
	180	90	90	80.71	131.21	188.53	245.57	299.83	350.75	405.09	447.43
			180	73.35	119.43	173.58	229.17	282.89	334	396.35	437.71
			270	64.26	105.83	156.93	211.34	264.76	316.3	387.4	427.75
			360	50.79	89.18	137.8	191.61	245.16	297.47	378.23	417.54
	270	135	135	73.23	112.66	156.53	202.4	245.2	285.27	330.71	364.64
			270	68.66	103.04	141.43	185.94	227.07	266.06	319.81	352.51
			405	63.39	91.93	124.01	167.59	207.17	245.21	308.51	339.93
			540	56.93	78.34	102.69	146.52	184.86	222.22	296.74	326.84
$f_{crd.A}$	90	45	45	110.93	181.23	270.73	342.4	410.55	472.12	545.23	601.23
			90	100.41	173.78	253.22	330.23	401.67	461.54	524.13	579.49
			135	93.76	162.46	243.45	318.45	381.65	453.43	504.26	557.64
			180	84.22	153.22	235.67	301.55	375.44	432.1	480.75	532.28
	180	90	90	85.74	137.69	193.56	240.33	290.45	336.7	392.56	434.59
			180	76.12	124.98	182.43	223.66	274.33	320.6	381.47	421.67
			270	67.89	109.14	162.11	207.65	258.04	299.6	368.25	412.68
			360	53.42	93.27	143.34	185.22	236.77	284.3	370.18	403.87
	270	135	135	77.66	117.91	165.55	180.88	234.87	271.45	315.68	351.85
			270	72.89	107.29	145.44	180.87	215.48	255.2	308.65	341.98
			405	67.65	95.33	129.56	161.33	198.59	231	294.38	330.29
			540	59.23	80.22	106.3	140.44	176.56	213.22	290.22	316.24
$f_{crd}/f_{crd.A}$	90	45	45	0.93	0.987	0.9728	1.0134	1.0345	1.0488	1.0211	1.0250
			90	0.9638	0.9732	0.9927	1.0137	1.0249	1.0394	1.0220	1.0229
			135	0.9561	0.9764	0.9805	1.0112	1.0432	1.0229	1.0187	1.0191
			180	0.9672	0.9608	0.9557	1.0238	1.0232	1.0352	1.0206	1.0196
	180	90	90	0.9413	0.953	0.974	1.0218	1.0323	1.0417	1.0319	1.0295
			180	0.9636	0.9556	0.9515	1.0246	1.0312	1.0418	1.0390	1.0380
			270	0.9465	0.9697	0.968	1.0177	1.026	1.0557	1.0520	1.0365
			360	0.9508	0.9562	0.9614	1.0345	1.0354	1.0463	1.0217	1.0338
	270	135	135	0.943	0.9555	0.9455	1.0479	1.0269	1.0509	1.0476	1.0364
			270	0.942	0.9604	0.9725	1.028	1.0538	1.0426	1.0362	1.0308
			405	0.937	0.9644	0.9572	1.0388	1.0432	1.0615	1.0480	1.0292
			540	0.9613	0.9766	0.966	1.0433	1.047	1.0422	1.0225	1.0335
Mean			1.0062								
Standard deviation			0.0375								
COV			0.0373								

Table 2. Comparison on distortional buckling stress between the proposed method and the finite element method for axial compression section with circular hole.

	h	d	a = 4.5	a = 9	a = 13.5	A = 18	a = 22.5	a = 27	a = 31.5	a = 36
f_{crd}	90	27	112.45	184.02	272.56	354.67	435.87	507.43	560.25	623.33
		45	103.17	178.87	263.36	346.98	424.71	495.14	546.71	612.74
		63	96.12	171.75	255.77	340.71	416.97	487.63	536.22	601.51
	180	54	89.75	138.77	195.92	251.81	307.86	361.88	404.05	446.95
		90	80.71	131.21	188.53	245.57	299.83	350.75	398.55	440.16
		126	73.67	124.62	181.66	240.09	292.34	341.57	392.35	433.25
	270	81	79.88	120.33	162.95	231.76	259.84	293.11	330.17	364.05
		135	73.23	112.66	156.53	202.4	245.2	285.27	322.57	355.59
		189	67.43	104.58	149.43	195.44	236.11	276.92	314.78	346.92
$f_{crd.A}$	90	27	116.71	188.57	276.45	344.59	413.27	489.65	548.25	615.78
		45	105.27	186.98	267.85	347.58	416.98	490.26	524.13	579.49
		63	98.95	180.57	259.64	341.57	414.63	480.36	504.26	557.64
	180	54	91.32	140.94	197.86	253.46	301.35	358.66	395.36	437.68
		90	86.22	137.69	198.47	250.98	298.61	345.2	387.56	434.59
		126	79.65	128.44	190.21	246.23	287.49	333.57	379.56	421.67
	270	81	83.61	125.67	167.89	230.84	255.68	284.75	319.22	355.35
		135	74.96	1193.27	159.37	200.34	246.23	279.52	305.81	342.68
		189	69.22	107.98	154.23	193.56	235.88	270.19	300.28	332.68
$f_{crd}/f_{crd.A}$	90	27	0.9635	0.9759	0.9859	1.0293	1.0547	1.0363	1.0219	1.0123
		45	0.9801	0.9566	0.9832	0.9983	1.0185	1.0100	1.0431	1.0574
		63	0.9714	0.9512	0.9851	0.9975	1.0056	1.0151	1.0634	1.0787
	180	54	0.9828	0.9846	0.9902	0.9935	1.0216	1.0090	1.0220	1.0212
		90	0.9361	0.9529	0.9499	0.9784	1.0041	1.0161	1.0284	1.0128
		126	0.9249	0.9703	0.9550	0.9751	1.0169	1.0240	1.0337	1.0275
	270	81	0.9554	0.9575	0.9706	1.0040	1.0163	1.0294	1.0343	1.0245
		135	0.9769	0.0944	0.9822	1.0103	0.9958	1.0206	1.0548	1.0377
		189	0.9741	0.9685	0.9689	1.0097	1.0010	1.0249	1.0483	1.0428
Mean			0.9893							
Standard deviation			0.1118							
COV			0.1130							

Table 3. Comparison on distortional buckling stress between the proposed method and the finite element method for bending section with rectangular hole.

	h	H_{hole}	L_{hole}	a = 4.5	a = 9	a = 13.5	a = 18	a = 22.5	a = 27	a = 31.5	a = 36
f_{crd}	270	135	135	92.62	153.48	220.58	285.64	346.59	403	455.03	503.32
			270	89.85	147.65	211.45	273.32	331.29	384.96	434.45	480.12
			405	86.94	141.53	201.83	260.35	315.19	365.97	412.81	456.03
			540	83.86	135.05	191.66	246.63	298.15	345.87	389.91	430.54
	360	180	180	82.65	132.49	187.65	241.21	291.43	337.95	380.87	420.47
			360	79.46	125.78	177.12	227.01	273.8	317.15	357.16	394.09
			540	76.04	118.56	165.8	211.73	254.83	294.78	331.66	365.7
			720	72.3	110.7	153.46	195.09	234.18	270.42	303.89	334.79
	450	225	225	78.84	124.5	175.1	224.2	270.4	313.1	352.54	388.95
			450	76.07	118.6	165.9	211.9	255	294.99	331.89	365.97
			675	73.1	112.4	156.1	198.6	238.6	275.6	309.78	341.36
			900	69.88	105.6	145.5	184.3	220.8	254.6	285.85	314.71
$f_{crd.A}$	270	135	135	98.67	162.55	231.55	290.51	351.42	408.25	451.08	487.69
			270	95.74	155.46	220.37	280.45	336.57	380.29	425.79	470.23
			405	90.23	149.78	215.47	264.71	320.46	358.77	400.29	443.79
			540	87.46	142.65	201.59	253.46	304.25	339.56	381.46	418.76
	360	180	180	86.23	139.89	193.56	246.77	296.44	336.7	367.92	405.68
			360	82.47	131.45	182.43	234.57	278.29	320.6	348.26	381.52
			540	80.75	127.65	175.46	216.85	261.33	299.6	315.78	351.49
			720	78.48	120.77	162.43	201.74	238.91	268.91	290.23	320.46
	450	225	225	83.94	131.78	187.24	230.49	276.48	321.65	338.97	362.57
			450	80.49	124.36	172.46	218.42	259.81	290.16	316.53	350.16
			675	78.54	120.36	163.58	204.63	245.36	271.85	294.38	328.46
			900	73.25	111.23	154.79	190.11	228.16	251.46	273.41	301.56
$f_{crd}/f_{crd.A}$	270	135	45	0.9387	0.9442	0.9526	0.9832	0.9863	0.9871	1.0088	1.0320
			90	0.9385	0.9498	0.9595	0.9746	0.9843	1.0123	1.0203	1.0210
			135	0.9635	0.9449	0.9367	0.9835	0.9836	1.0201	1.0313	1.0276
			180	0.9588	0.9467	0.9507	0.9731	0.9800	1.0186	1.0222	1.0281
	360	180	90	0.9585	0.9471	0.9695	0.9775	0.9831	1.0037	1.0352	1.0365
			180	0.9635	0.9569	0.9709	0.9678	0.9839	0.9892	1.0256	1.0329
			270	0.9417	0.9288	0.9449	0.9764	0.9751	0.9839	1.0503	1.0404
			360	0.9213	0.9166	0.9448	0.9670	0.9802	1.0056	1.0471	1.0447
	450	225	135	0.9392	0.9448	0.9352	0.9727	0.9780	0.9734	1.0400	1.0728
			270	0.9451	0.9537	0.9620	0.9701	0.9815	1.0166	1.0485	1.0452
			405	0.9307	0.9339	0.9543	0.9705	0.9724	1.0138	1.0523	1.0393
			540	0.9540	0.9494	0.9400	0.9694	0.9677	1.0125	1.0455	1.0436
Mean				0.9840							
Standard deviation				0.0378							
COV				0.0384							

Table 4. Comparison on distortional buckling stress between the proposed method and the finite element method for bending section with circular hole.

	h	d_{hole}	a = 4.5	a = 9	a = 13.5	a = 18	a = 22.5	a = 27	a = 31.5	a = 36
f_{crd}	270	81	93.15	162.78	222.36	301.44	349.56	409.35	462.03	522.64
		135	92.62	153.48	220.58	285.64	346.59	403.02	455.03	503.32
		189	86.53	141.23	212.69	268.96	333.37	390.42	437.26	489.27
	360	108	84.61	142.65	194.13	257.23	302.29	350.14	395.46	436.72
		180	82.65	132.49	187.65	241.21	291.43	337.95	380.87	420.47
		252	81.16	125.63	182.72	230.47	283.18	325.46	369.77	408.12
	450	135	79.91	128.66	178.58	229.56	276.25	320.45	360.45	397.75
		225	78.84	124.5	175.1	224.2	270.4	313.1	352.54	388.95
		315	77.75	117.85	171.47	215.98	264.34	305.62	344.44	379.93
$f_{crd.A}$	270	81	100.42	174.56	231.07	311.27	353.24	410.22	460.22	510.28
		135	98.52	161.29	228.97	296.38	350.16	405.27	451.26	488.71
		189	91.84	150.74	221.08	275.84	339.84	394.85	432.77	471.26
	360	108	87.98	152.43	203.46	264.85	309.55	353.67	391.59	423.47
		180	85.74	141.28	200.38	251.73	300.75	354.79	378.66	408.33
		252	85.47	131.04	191.28	240.22	289.71	340.28	364.92	400.11
	450	135	84.56	135.26	185.79	236.75	284.53	329.11	357.84	382.51
		225	84.08	130.87	182.44	232.82	278.39	317.54	350.07	372.54
		315	82.56	123.59	180.28	224.66	271.88	309.62	340.73	367.23
$f_{crd}/f_{crd.A}$	270	81	0.9276	0.9325	0.9623	0.9684	0.9896	0.9979	1.0039	1.0242
		135	0.9401	0.9516	0.9634	0.9638	0.9898	0.9944	1.0084	1.0299
		189	0.9422	0.9369	0.9620	0.9751	0.9810	0.9888	1.0104	1.0382
	360	108	0.9617	0.9358	0.9541	0.9712	0.9765	0.9900	1.0099	1.0313
		180	0.9640	0.9378	0.9365	0.9582	0.9690	0.9525	1.0058	1.0297
		252	0.9496	0.9587	0.9552	0.9594	0.9775	0.9564	1.0133	1.0200
	450	135	0.9450	0.9512	0.9612	0.9696	0.9709	0.9737	1.0073	1.0398
		225	0.9377	0.9513	0.9598	0.9630	0.9713	0.9860	1.0071	1.0440
		315	0.9417	0.9536	0.9511	0.9614	0.9723	0.9871	1.0109	1.0346
Mean			0.9765							
Standard deviation			0.0304							
COV			0.0311							

Table 5. Statistic of comparison on distortional buckling stress between the proposed method and the finite element method.

	Axial compression members		bending members	
	Circular hole	Rectangular hole	Circular hole	Rectangular hole
Count	72	96	72	96
Mean	0.9893	1.0062	0.9765	0.9840
Standard deviation	0.1118	0.0375	0.0304	0.0378
COV	0.1130	0.0373	0.0311	0.0384
Mean	0.9990		0.9808	
Standard deviation	0.0692		0.0346	
COV	0.0693		0.0353	
Mean	0.9899			
Standard deviation	0.0519			
COV	0.0524			

3. EWM-based design method for distortional buckling strength

The effective width method is used to calculate the sectional strength of CFS member considering the local buckling in Chinese code. The design formula of effective width is derived from Eq (15) which is obtained from the test results conducted in China.

$$b_e = \left[\left(0.6\sigma_{crd} / f_y\right)^{1/4} - 0.1\right] b \tag{15}$$

where σ_{crd} is the buckling stress of plate, f_y is the yield strength of steel.

Equation (15) can be rewritten as Eq (16) for sectional strength.

$$\frac{P_{crd}}{P_y} = \frac{A_e f_y}{A f_y} = \frac{b_e t}{b t} = \left[\left(\frac{0.6\sigma_{crd}}{f_y}\right)^{1/4} - 0.1\right] \tag{16}$$

Substituting E = 206000 N/mm^2 and v = 0.3 in equation $\sigma_{crd} = kE\pi^2 / \left(12(1-v^2)\right)(t/b)^2$ and considering $\rho = \sqrt{235k / f_y}$, the effective width formula can be obtained from Eq (15) as Eq (17).

$$b_e = \left(\sqrt{21.8\rho t / b} - 0.1\right) b \tag{17}$$

The plate would be all effective if the effective width (b_e) calculated by using Eq (17) is larger or equal to the width of plate (b). Then the Eq (18) should be demanded.

$$\left(\sqrt{21.8\rho t / b} - 0.1\right) \geq 1 \tag{18}$$

The Eq (19) can be obtained from Eq (18).

$$b / t \leq 18\rho \tag{19}$$

Based on Eqs (17) and (19) and consideration that the effective width is the constant value when the width-to-thickness ratio of the plate is larger or equal to 38ρ, Eq (20) is presented to calculate the effective width for CFS section [28]. Herein, Eq (20) is also proposed to calculate the effective width of CFS lipped channel section with holes for considering distortional buckling.

$$\frac{b_e}{t}=\begin{cases}\dfrac{b_c}{t} & \dfrac{b}{t}\le 18\alpha\rho \\ \left(\sqrt{\dfrac{21.8\alpha\rho}{\frac{b}{t}}}-0.1\right)\dfrac{b_c}{t} & 18\alpha\rho<\dfrac{b}{t}<38\alpha\rho \\ \dfrac{25\alpha\rho}{\frac{b}{t}}\dfrac{b_c}{t} & \dfrac{b}{t}\ge 38\alpha\rho\end{cases} \tag{20}$$

where b_c is the compression width of the plate, α is the coefficient, α=1.15-0.15ψ, ψ is the uneven distribution coefficient of the compression stress, $\psi=\sigma_{\max}/\sigma_{\min}$, $\sigma_{\max}$ and $\sigma_{\min}$ are the maximum compression stress and the minimum compression stress or the tension stress for the calculated plate.

In the equation $\rho=\sqrt{235k/f_y}$, k is the buckling coefficient of the plate. Considering expression $\sigma=kE\pi^2/\left(12(1-\nu^2)\right)(t/b)^2$, the distortional buckling coefficient k for the flange can be obtained from Eqs (21) and (22) based on Eqs (9), (11) and (13).

If the maximum compression stress acts at the stiffened edge (web):

$$k=\frac{\left(1-\frac{L_{hole}}{L}\right)(2+\alpha_w)\frac{L^2}{\pi^4}+b\left[(b/L)^2/3+2(1-\nu)/\pi^2\right]+12(1-\nu^2)I(b/L)^2/t^3}{b(1/3-\alpha/12)+a} \tag{21}$$

If the maximum compression stress acts at the unstiffened edge (lip):

$$k=\frac{\left(1-\frac{L_{hole}}{L}\right)(2+\alpha_w)\frac{L^2}{\pi^4}+b\left[(b/L)^2/3+2(1-\nu)/\pi^2\right]+12(1-\nu^2)I(b/L)^2/t^3}{b(1/3-\alpha/4)+a(1-\alpha)} \tag{22}$$

where, I is the moment of inertia of lip about the central axis of the lip and the flange.

For the flange of CFS lipped channel section, the buckling coefficient can be calculated by using Eq (23) if the local buckling is considered.

If the maximum compression stress acts at the stiffened edge (web):

$$k=\min\left(2\alpha^3+2\alpha+4,\frac{\left(1-\frac{L_{hole}}{L}\right)(2+\alpha_w)\frac{L^2}{\pi^4}+b\left[(b/L)^2/3+2(1-\nu)/\pi^2\right]+12(1-\nu^2)I(b/L)^2/t^3}{b(1/3-\alpha/12)+a}\right) \tag{23a}$$

If the maximum compression stress acts at the unstiffened edge (lip):

$$k=\begin{cases}\min\left(2\alpha^3+2\alpha+4,\dfrac{\left(1-\dfrac{L_{hole}}{L}\right)\left(2+\alpha_w\right)\dfrac{L^2}{\pi^4}+b\left[\left(b/L\right)^2/3+2\left(1-\nu\right)/\pi^2\right]+12(1-\nu^2)I\left(b/L\right)^2/t^3}{b\left(1/3-\alpha/4\right)+a\left(1-\alpha\right)}\right) & \alpha<\dfrac{b/3+a}{b/4+a}\\ 2\alpha^3+2\alpha+4 & \alpha\geq\dfrac{b/3+a}{b/4+a}\end{cases} \tag{23b}$$

where, L is the minimum of distortional buckling half wavelength calculated by using Eq (14) and the effective length of CFS member.

4. Ultimate strength of distortional buckling and interaction buckling

4.1. Design method

4.1.1. Novel effective width method

The design formula of ultimate capacity for CFS lipped channel axial compression member with holes is shown as follow:

$$N_u=\varphi_{hole}A_{ehole}f_y \tag{24}$$

where, φ_{hole} is the overall buckling coefficient which can be calculated by using weighted average method in AISI S100 considering the effect of the hole, A_{ehole} is the effective section area of the axial compression member considering the effect of the hole which can be obtained from the effective width of the axial compression member with holes calculated by using Eq (20). When the Eq (20) is used to calculate the effective width of CFS lipped channel section with holes, the buckling coefficient k in the equation $\rho=\sqrt{235k/f_y}$ can be obtained as follows: The buckling coefficient k of the stiffened element (web) considering the effect of the hole should be calculated according to the reference [18]. The buckling coefficient k of the partially stiffened element (flange) considering the effect of the hole should be calculated by using Eq (23). The buckling coefficient k of the unstiffened element (lip) ignoring the effect of the hole can be predicted according to Chinese code GB50018 [28].

For CFS lipped channel bending member with holes, the ultimate capacity can be calculated as follow:

$$M_u=\varphi_{bhole}W_{ehole}f_y \tag{25}$$

where φ_{bhole} is the overall flexual-torsional buckling coefficient which can be calculated by using weighted average method in AISI S100 considering the effect of the hole, W_{ehole} is the effective section modulus of the bending member considering the effect of the hole which can be obtained from the effective width of the bending member with holes calculated by using Eq (20). When the Eq (20) is used to calculate the effective width of CFS lipped channel section with holes, the buckling coefficient k in the equation $\rho=\sqrt{235k/f_y}$ can be obtained as follows: The buckling coefficient k of the stiffened element (web) considering the effect of the hole can be predicted by using the modified method in reference [18]. The buckling coefficient k of the partially stiffened element (flange) considering the effect of the hole should be calculated by using Eq (23). The buckling coefficient k of the unstiffened element (lip) ignoring the effect of the hole can be

calculated according to Chinese code GB50018 [28].

4.1.2. Direct strength method in North America code

AISI S100 presents a direct strength method (DSM) to calculate the ultimate strength of CFS lipped channel section with holes. The ultimate capacity P_n of axial compression column with holes is the least of the interaction buckling capacity of global buckling and local buckling and the distortional buckling capacity, i.e., $P_n = \min(P_{n\ell}, P_{nd})$. The expressions of the buckling capacity for axial compression column with holes are displayed as follows:

The local buckling capacity, $P_{n\ell}$, should be calculated in accordance with Eq (26).

$$P_{nl} = \begin{cases} P_{ne} & \lambda_l \le 0.776 \\ \left[1 - 0.15\left(\frac{P_{crl}}{P_{ne}}\right)^{0.4}\right]\left(\frac{P_{crl}}{P_{ne}}\right)^{0.4} P_{ne} & \lambda_l > 0.776 \end{cases} \tag{26}$$

where $\lambda_l = \sqrt{P_{ne} / P_{crl}}$, P_{crl} is the critical elastic local buckling capacity considering the influence of the hole which can be obtained from the finite element analysis. P_{ne} is the global buckling capacity defined as expression (27).

$$P_{ne} = \begin{cases} (0.658^{\lambda_c^2})P_y & \lambda_c \le 1.5 \\ (\frac{0.877}{\lambda_c^2})P_y & \lambda_c > 1.5 \end{cases} \tag{27}$$

where $\lambda_c = \sqrt{P_y / P_{cre}}$, P_y is the yield strength, $P_y = Af_y$; P_{cre} is the elastic global buckling capacity, $P_{cre} = Af_{cre}$, f_{cre} is the least of the applicable elastic global (flexural, torsional, or flexural-tortional) buckling stress.

The distortional buckling capacity for the axial compression column with holes, P_{nd}, should be calculated as follow:

$$P_{nd} = \begin{cases} P_{ynet} & \lambda_d \le \lambda_{d1} \\ P_{ynet} - \left(\frac{P_{ynet} - P_{d2}}{\lambda_{d2} - \lambda_{d1}}\right)(\lambda_d - \lambda_{d1}) & \lambda_{d1} < \lambda_d \le \lambda_{d2} \end{cases} \tag{28}$$

where $\lambda_d = \sqrt{P_y / P_{crd}}$, $P_{d2} = \left[1 - 0.25\left(\frac{1}{\lambda_{d2}}\right)^{1.2}\right]\left(\frac{1}{\lambda_{d2}}\right)^{1.2} P_y$, $\lambda_{d1} = 0.561\left(\frac{P_{ynet}}{P_y}\right)$, $\lambda_{d2} = 0.561\left(14\left(\frac{P_y}{P_{ynet}}\right)^{0.4} - 13\right)$, P_{ynet} is the yield strength of the net-section, $P_{ynet} = A_{net}f_y$, P_{crd} is the critical elastic distortional buckling capacity considering the effect of the hole which can be obtained from the weight average method in AISI or finite element analysis. It is worth noting that the calculated P_{nl} and P_{nd} as expressed above should be less than P_{ynet}.

The DSM equations used to predict the nominal ultimate strength of bending member with holes can be found in AISI S100 [27].

4.2. Test data and validated of proposed method

Historically, many axial compression experiments [8−19] and a small number of bending tests [20,21]

on CFS channel members with circular holes, rectangular holes, or slotted holes were conducted. Results obtained from these studies were assembled in a database to validate the proposed EWM-based design expressions for CFS lipped channel member with holes in this paper. The experimental database includes 319 axial compression specimens and 28 beam specimens. These specimens displayed different buckling modes including the distortional buckling and the interaction buckling. The dimensions of the cross-section and the hole included in the database are provided in Table 6.

Table 6. The dimensions of the section and the hole of test specimens.

Load type	Refe--rence	count	*h/t*	*h/b*	*a/t*	Circular hole	Rectangular hole	Slotted hole
						d/h	L_{hole}/h	L_{hole}/h
Axial compression members	[8]	32	49, 76	2.1	8, 12	0.135, 0.27, 0.4		
	[9]	42	62, 122	2.07, 3.39	10, 12	0.17, 0.34, 0.5, 0.55, 0.65, 1		
	[10]	16	45, 60, 75, 90	1, 1, 2, 1, 5, 2	10, 12	0.1, 0.3, 0.5, 0.7		
	[11]	12	105, 155	1.9, 3.2	17			0.62, 0.95
	[12]	16	108, 133	3.1, 3.2	14, 16.5			0.46, 0.7, 0.8
	[13]	37	50, 175	2.35, 4	7.5, 12		0.25, 0.4	
	[14]	14	80, 110	2.3, 4.3	9, 12.25		0.3, 0.35, 0.55, 0.95	
	[15]	30	87, 127	1.8	15, 6, 22.6		0.13, 0.17, 0.25, 0.34	
	[16]	6	64	2.7	8		0.32, 0.44	
	[17]	44	100	1.1, 1.3	10, 12.5		0.4, 0.8, 1.2	
	[18]	28	100, 112.5	1.1, 1.8	10, 18.75	0.3, 0.5, 0.7	0.4, 0.8, 1.2	
	[19]	42	75, 93.75, 100, 112.5	1.33, 1.8, 1.88	10, 12.5, 18.75	0.3, 0.5, 0.7	0.4, 0.8, 1.2	
Bending members	[20]	16	100	200/80	10, 20		0.5	
	[21]	12	203/1.78	203/63			152/203	

Due to space limitations, only the ultimate capacities predicted by using the proposed method and direct strength method in North America code (AISI100 2016) for axial compression members in reference [18] and bending members in reference [20] are presented in Tables 7 and 8, where P_t is the test results, P_{EWM} and P_N are the calculated results by using the proposed EWM and North America code, respectively. M_t is the test results, M_{EWM} and M_N are the calculated results by using the proposed EWM and North America code, respectively.

Table 7. Comparison on ultimate strength between tests and predicted results using AISI and proposed EWM for axial compression members in reference [18].

Specimen	P_t/KN	P_{EWM}/KN	P_N/KN	P_t/P_{EWM}	P_t/P_N
C8008-05-RH21-1	34.55	32.80	36.25	1.05	0.95
C8008-05-RH21-2	34.4	32.38	35.62	1.06	0.97
C8008-05-RH41-1	33.3	31.28	34.98	1.06	0.95
C8008-05-RH41-2	33.91	30.59	34.44	1.11	0.98
C8008-05-RH61-1	29.91	29.30	32.14	1.02	0.93
C8008-05-RH61-2	29.45	29.26	31.41	1.01	0.94
C10010-05-RH21-1	51.95	49.32	53.54	1.05	0.97
C10010-05-RH21-2	51.48	49.40	53.06	1.04	0.97
C10010-05-RH41-1	51.1	48.51	53.76	1.05	0.95
C10010-05-RH41-2	50.22	48.69	52.29	1.03	0.96
C10010-05-RH61-1	46.19	43.39	49.63	1.06	0.93
C10010-05-RH61-2	44.12	43.67	46.42	1.01	0.95
C8008-10-RH21-1	27.5	26.13	29.28	1.05	0.94
C8008-10-RH21-2	27.74	26.09	28.19	1.06	0.98
C8008-10-RH41-1	26.94	24.30	27.54	1.11	0.98
C8008-10-RH41-2	26.33	24.39	27.25	1.08	0.97
C8008-10-RH61-1	23.8	22.96	24.44	1.04	0.97
C8008-10-RH61-2	23.88	23.12	24.23	1.03	0.99
C8008-10-RH22-1	27.6	25.79	29.52	1.07	0.93
C8008-10-RH22-2	27.3	25.95	28.07	1.05	0.97
C8008-10-RH42-1	26.52	24.15	27.31	1.10	0.97
C8008-10-RH42-2	25.89	23.84	27.77	1.09	0.93
C8008-10-RH62-1	23.5	22.67	24.26	1.04	0.97
C8008-10-RH62-2	23.47	22.89	23.65	1.03	0.99
C10010-10-RH21-1	40.1	40.04	42.03	1.00	0.95
C10010-10-RH21-2	40.95	40.08	43.06	1.02	0.95
C10010-10-RH41-1	39.38	37.16	40.30	1.06	0.98
C10010-10-RH41-2	39.4	37.08	40.65	1.06	0.97
C10010-10-RH61-1	37.3	35.88	37.88	1.04	0.98
C10010-10-RH61-2	37.66	36.19	39.46	1.04	0.95
C10010-10-RH22-1	40.25	39.95	41.39	1.01	0.97
C10010-10-RH22-2	41.03	40.55	42.93	1.01	0.96
C10010-10-RH42-1	38.45	37.53	39.27	1.02	0.98
C10010-10-RH42-2	38.7	37.90	40.84	1.02	0.95
C10010-10-RH62-1	36.8	36.44	35.72	1.01	1.03
C10010-10-RH62-2	37.05	36.30	37.24	1.02	0.99
Mean				1.0454	0.9646
Standard deviation				0.0286	0.0211
COV				0.0273	0.0219
β				2.97	2.54

Table 8. Comparison on ultimate strength between tests and predicted results by using AISI and proposed EWM for bending members in reference [20].

Specimen	M_t/KN.m	M_{EWM}/KN.m	M_N/KN.m	M_t/M_{EWM}	M_t/M_N
H200r0.2d20t2.0	14.315	13.54	15.11	1.0572	0.9474
H200r0.4d20t2.0	14.168	13.54	15.09	1.0464	0.9389
H200r0.6d20t2.0	13.800	13.54	15.04	1.0192	0.9176
H200r0.8d20t2.0	13.271	13.54	13.82	0.9801	0.9603
H200r0.2d40t2.0	16.684	14.86	18.24	1.1227	0.9147
H200r0.4d40t2.0	16.333	14.86	18.14	1.0991	0.9004
H200r0.6d40t2.0	15.154	14.86	17.97	1.0198	0.8433
H200r0.8d40t2.0	14.565	14.86	17.68	0.9801	0.8238
Mean				1.0406	0.9058
Standard deviation				0.0483	0.0456
COV				0.0464	0.0504
β				2.71	2.44

Reliability analysis was conducted to assess the appropriateness of the proposed EWM method. The target reliability index(β) for CFS structural members is 2.5 for Load and Resistance Factor Design (LRFD) according to the NAS (AISI S100-16) [27]. The resistance factor ϕ_c and ϕ_b for the axial compression member and the bending member are 0.80 and 0.90 as specified in the NAS (AISI S100-16) [27], respectively. The dead load and live load factors are 1.2 and 1.6, respectively. The ratio of nominal dead load to nominal live load is 0.2. The mean value of the fabrication factor(F_M) is 1.00 and coefficients of variation of fabrication factor (V_F) is 0.05. The mean value of the material factor (M_M) is 1.10 and coefficients of variation of material factor (V_M) is 0.10. The reliability index were calculated using the load combination of 1.2 DL + 1.6 LL for axial compression members in reference [18] and bending members in reference [20] as shown in Tables 7 and 8.

For axial compression members as shown in Table 7, the mean values of P_t/P_{EWM} and P_t/P_N are 1.0454 and 0.9646 with the corresponding coefficient of variations of 0.0273 and 0.0219 and the calculated reliability indexes are 2.97 and 2.54, respectively. The comparisons show that the modified effective width method displays a great accuracy and variation. All the reliability indices are larger than 2.5 and the reliability index of the modified effective width method is higher than that of the direct strength method in North America code.

For bending members as shown in Table 8, the mean values of M_t/M_{EWM} and M_t/M_N are 1.0406 and 0.9058 with the corresponding coefficient of variations of 0.0464 and 0.0504 and the calculated reliability indexes are 2.71 and 2.44, respectively. The comparisons show that the modified effective width method displays a great accuracy and variation. The reliability index of the modified effective width method is larger than 2.5 and the reliability index of the direct strength method in North America code is less than 2.5 which indicates that the direct strength method in North America code has a sligth unsafe for the bending members in reference [20].

The statistical results and reliability analysis results about the comparison on ultimate strength between the predicted results and test results are listed in Table 9 for all specimens shown in Table 6. As shown in Table 9, the calculated reliability indexes of P_t/P_{EWM} and P_t/P_N are 2.82 and 2.61,

respectively. The calculated reliability indexes of M_t/M_{EWM} and M_t/M_N are 2.66 and 2.51, respectively. The proposed effective width method provides a good agreement with the test results and the higher reliability index.

Table 9. Comparison on ultimate strength between tests and predicted results.

	Axial compression members		Bending members	
	P_t/P_{EWM}	P_t/P_N	M_t/M_{EWM}	M_t/M_N
Mean	1.0269	0.9724	1.0247	0.9137
Standard deviation	0.0489	0.0884	0.036	0.0433
COV	0.0476	0.0909	0.0351	0.0474
β	2.82	2.61	2.66	2.51

4.3. Validation of proposed method with finite element analysis

In order to further verify the novel EWM-based design method of the distortional buckling and interaction buckling, CFS lipped channel sections were selected to get ultimate strengths by using proposed effective width method and finite element method. The section dimensions included the thickness of 2 mm, the width of flanges of 90 mm, the ratios of width of lip to width of flange of 0.05, 0.1, 0.15, 0.2, 0.25, 0.3, 0.35 and 0.4, and the width of the web of 90 mm,180 mm and 270 mm for axial compression members and 270 mm, 360 mm and 450 mm for bending members. The ratios of the diameter of the circular hole to the width of the web are 0.3, 0.5 and 0.7. The ratio of height of the rectangular hole to the width of the web is 0.5, the length-to-height ratios of the rectangular hole are 1, 2, 3 and 4. The slenderness ratio of axial compression member is 15, 45, 75, 100 and 120. The relative slenderness ratio $\bar{\lambda} = \sqrt{M_p / M_e}$ for the bending member is 0.5, 0.7, 0.9, 1.1 and 1.3. The total of members is 1260 including 270 axial compression members with circular hole, 360 axial compression members with rectangular hole, 270 bending members with circular hole, and 360 bending members with rectangular hole.

The statistical results and reliability analysis results of the ratios of the ultimate strength calculated by using the proposed effective width method and direct strength method in North America code and finite element analysis results are shown in Table 10. The mean values of P_A/P_{EWM} and P_A/P_N are 1.0377 and 0.9784 with the corresponding coefficient of variations of 0.0387 and 0.043 and the calculated reliability indexes are 2.86 and 2.63, respectively. The mean values of M_A/M_{EWM} and M_A/M_N are 1.0289 and 0.9693 with the corresponding coefficient of variations of 0.0405 and 0.0509 and the calculated reliability indexes are 2.68 and 2.55, respectively. The comparisons show that the modified effective width method displays a great accuracy and variation. All the reliability indices are larger than 2.5 and the reliability index of the modified effective width method is higher than that of the direct strength method in North America code.

Table 10. Comparison on ultimate capacity between the predicted results and finite element results.

	Axial compression members		Bending members	
	P_A/P_{EWM}	P_A/P_N	M_A/M_{EWM}	M_A/M_N
Mean	1.0377	0.9784	1.0289	0.9693
Standard deviation	0.0402	0.0421	0.0417	0.0493
COV	0.0387	0.0430	0.0405	0.0509
β	2.86	2.63	2.68	2.55

Meanwhile, the sections selected from the steel stud manufacturers association (SSMA) including 213 axial compression columns and 125 bending members with slotted holes or circular holes were also analyzed by using finite element software to further verify the novel EWM-based design method. Due to space limitations, the details of sections cannot be provided in this paper, which can be found in reference [43].

The statistical results and reliability analysis results of the ratios of ultimate strength calculated using proposed effective width method and direct strength method in North America code and finite element analysis results are shown in Table 11. The calculated reliability indexes of P_A/P_{EWM} and P_A/P_N are 2.82 and 2.61, respectively. The calculated reliability indexes of M_A/M_{EWM} and M_A/M_N are 2.66 and 2.51, respectively. The comparisons show that the modified effective width method displays a great accuracy and variation. All the reliability indices are larger than 2.5 and the reliability index of the modified effective width method is higher than that of the direct strength method in North America code.

Table 11. Comparison on ultimate capacity between the predicted results and finite element results.

	Axial compression members		Bending members	
	P_A/P_{EWM}	P_A/P_N	M_A/M_{EWM}	M_A/M_N
Mean	1.0106	0.9608	1.0065	0.9716
Standard deviation	0.0452	0.0441	0.0590	0.0484
COV	0.0447	0.0459	0.0586	0.0498
β	2.75	2.61	2.64	2.59

5. Conclusions

The calculated methods of the elastic distortional buckling stress and buckling coefficient of CFS lipped channel section with holes were developed by using the energy method and simplified rotation restrain stiffness in this paper. The mean value of the ratios of distortional buckling stress between the predicted results and finite element results was 0.9899 with the corresponding coefficient of variation of 0.0524 for 336 CFS lipped channel members. The statistical result of the comparison on distortional buckling stress showed the proposed method had a very high precision. Based on the proposed distortional buckling coefficient of CFS lipped channel section with holes, this paper presented an EWM-based design method to calculate the distortional buckling strength and interaction buckling strength of CFS lipped channel section with holes. The proposed method was validated by 347 test results and 1598 finite element analysis results. Meanwhile, the direct strength method in North America specification was also used to predict the ultimate strength of CFS lipped

channel section with holes. The statistical results and reliability analysis results about the comparison on ultimate strength between the predicted results and test results or finite element analysis results were performed. The comparisons showed that the modified effective width method displayed a great accuracy and variation. All the reliability indices were larger than 2.5 and the reliability index of the modified effective width method was higher than that of the direct strength method in North America code. The reliability index of axial compression members is higher than that of bending members. The reliability index of the direct strength method in North America code is less than 2.5 for the bending members in reference [20] which indicates that the direct strength method in North America code has a slight unsafe for some bending members. Thus the proposed effective width method allows designers to calculate the ultimate capacity of CFS lipped channel member with holes by using the existing design method in Chinese specification with simplified modifications.

Conflict of interest

The author declares that there is no conflict of interest regarding the publication of this paper.

Acknowledgments

The author gratefully thanks the financial support provided by National Natural Science Foundation Projects of China (grant number 51868049).

References

1. S. C. W. Lau, G. J. Hancock, Distortional buckling formulas for channel columns, *J. Struct. Eng.*, **113** (1987), 1063−1078. doi: 10.1061/(ASCE)0733-9445(1987)113:5(1063).
2. Y. B. Kwon, G. J. Hancock, Tests of cold-formed channels with local and distortional buckling. *J. Struct. Eng.,***118** (1992), 1786−1803. doi:10.1061/(ASCE)0733-9445(1992)118:8(1786).
3. G. J. Hancock, Design for distortional buckling of flexural members, *Thin walled Struct.*,**27** (1997), 3−12. doi:10.1016/0263-8231(96)00020-1.
4. B. W. Schafer, T. Pekoz, Laterally braced cold-formed steel flexural members with edge stiffened flanges, *J. Struct. Eng.*, **125** (1999), 118−127. doi:10.1061/(ASCE)0733-9445(1999)125:2(118).
5. B. W. Schafer, Local, distortional, and euler buckling of thin-walled columns, *J. Struct. Eng.*, **128** (2002), 289−299. doi:10.1061/(ASCE)0733-9445(2002)128:3(289).
6. X. Yao, *Distortional buckling behavior and design method of cold-formed thin-walled steel sections*, Tongji University, 2012.
7. X. Yao, Y. Li, Distortional buckling strength of cold-formed thin-walled steel members with lipped channel section, *Eng. Mech.*, **31** (2014), 174−181. doi: 1000-4750(2014)09-0174-08.
8. R. A. Ortiz-Colberg, *The load carrying capacity of perforated cold-formed steel columns*, Cornell University, (1981), 152.
9. K. S. Sivakumaran. Load capacity of uniformly compressed cold-formed steel section with punched web, *Can. J. Civ. Eng.*, **14** (1987), 550−558. doi: 10.1139/l87-080.
10. B. He, G. Zhao, Analysis on buckling behavior of cold-formed lipped channel with perforated web, *J. Xi'an Inst. Met. Const. Eng.*, **21** (1989), 1−9.

11. C. D. Moen, B. W. Schafer, Experiments on cold-formed steel columns with holes, *Thin Walled Struct.*, **46** (2008), 1164−1182. doi: 10.1016/j.tws.2008.01.021.
12. L. Xu, Y. Shi, S. Yang, Compressive strength of cold-formed steel c-shape columns with slotted holes, in *Twenty-second international specialty conference on cold-formed steel structures: recent research and developments in cold-formed steel design and construction*, (2014). Available from: https://scholarsmine.mst.edu/isccss/22iccfss/session02/4/.
13. T. H. Miller, T. Pekoz, Unstiffened strip approach for perforated wall studs, *J. Struct. Eng.*, **120** (1994), 410−421. doi: 10.1061/(ASCE)0733-9445(1994)120:2(410).
14. N. Abdel-Rahman, Cold-formed steel compression members with perforations, PhD thesis, Mc Master University, Hamilton, Ontario, 1997.
15. Y. Pu, M. H. R. Godley, R. G. Beale, H. Lau, Prediction of ultimate capacity of perforated lipped channels, *J. Struct. Eng.*, **125** (1999), 510−514. doi: 10.1061/(ASCE)0733-9445(1999)125:5(510).
16. B. Hu, Y. Liu, Ultimate capacities of cold-formed thin-walled channel columns with single hole under axial compression, *J. Jiangsu Univ.*, **28** (2007), 258−261. doi: CNKI:SUN:JSLG.0.2007-03-018.
17. Y. Guo, X. Yao, Distortional buckling behavior and design method of cold-formed steel lipped channel with rectangular holes under axial compression, *Math. Bios. Eng.*, **18** (2021), 6239−6261. doi: 10.3934/mbe.2021312.
18. Y. Guo, X. Yao, Experimental study and effective width method for cold-formed steel lipped channel stud columns with holes, *Adv. Civil Eng.*, **2021** (2021), 9949199. doi:10.1155/2021/9949199.
19. X. Yao, Experimental investigation and load capacity of slender cold-formed lipped channel sections with holes in compression, *Adv. Civil Eng.*, **2021** (2021), 6658099. doi:10.1155/2021/6658099.
20. J. Zhao, K. Sun, C. Yu, J. Wang. Tests and direct strength design on cold-formed steel channel beams with web holes. *Eng. Struct.*, **184** (2019), 434−446. doi: 10.1016/j.engstruct.2019.01.062.
21. C. D. Moen, A. Schudlich, A. Heyden, Experiments on cold-formed steel C-section joists with unstiffened web holes, *J. Struct. Eng.*, **139** (2013), 695−704. doi: 10.1061/(ASCE)ST.1943-541X.0000652.
22. J. Zhou, S. Yu, Equiavalentcal calculation of buckling stress for cold-formed thin wall perforated channel columns, *Steel. Const.*, **25** (2010), 27−31.
23. C. D. Moen, B. W. Schafer, Elastic buckling of cold-formed steel columns and beams with holes, *Eng. Struct.*, **31** (2009), 2812−2824. doi: 10.1016/j.engstruct.2009.07.007.
24. X. Yao, Y. Guo, Y. Liu, J. Su, Y. Hu, Analysis on distortional buckling of cold-formed thin-walled steel lipped channel steel members with web openings under axial compression, *Indust. Const.*, **50** (2020), 170−177. doi: 1000-4750(2014)09-0174-08.
25. C. D. Moen, B. W. Schafer, Direct strength method for design of cold-formed steel columns with holes, *J. Struct. Eng.*, **137** (2016), 559−570. doi: 10.1061/(ASCE)ST.1943-541X.0000310.
26. Z. Yao, K. J. R. Rasmussen, Perforated cold-formed steel members in compression. II: Design, *J. Struct. Eng.*, **143** (2017), 04016227. doi:10.1061/(ASCE)ST.1943-541X.0001636.
27. American Iron and Steel Institute, *North American specification for the design of cold-formed steel structural members*, *Canadian Standards Association*, (2001). Available from: https://www.ce.jhu.edu/cfs/cfslibrary/AISI-S100-07%20Commentary.pdf.

28. Ministry of Housing and Urban-Rural Development of the People's Republic of China, *Technical code for cold-formed thin-walled steel structures*, Chinese Planning Press, (2002).
29. A. Uzzaman, J. B. P. Lim, D. Nash, J. Rhodes, B. Young, Cold-formed steel sections with web openings subjected to web crippling under two-flange loading conditions-part I: tests and finite element analysis, *Thin Walled Struct.*, **56** (2012), 38−48. doi: 10.1016/j.tws.2012.03.010.
30. A. Uzzaman, J. B. P. Lim, D. Nash, J. Rhodes, B. Young, Cold-formed steel sections with web openings subjected to web crippling under two-flange loading conditions-Part II: parametric study and proposed design equations, *Thin Walled Struct.*, **56** (2012), 79−87. doi: 10.1016/j.tws.2012.03.009.
31. Y. Lian, A. Uzzaman, J. B. Lim, G. Abdelal, D. Nash, B. Young, Effect of web holes on web crippling strength of cold-formed steel channel sections under end-one-flange loading condition-Part I: Tests and finite element analysis, *Thin Walled Struct.*, **107** (2016), 443−452. doi: 10.1016/j.tws.2016.06.025.
32. Y. Lian, A. Uzzaman, J. B. Lim, G. Abdelal, D. Nash, B. Young, Effect of web holes on web crippling strength of cold-formed steel channel sections under end-one-flange loading condition-Part II: Parametric study and proposed design equations, *Thin Walled Struct.*, **107** (2016), 489−501. doi: 10.1016/j.tws.2016.06.026.
33. Y. Lian, A. Uzzaman, J. B. Lim, G. Abdelal, D. Nash, B. Young, Web crippling behaviour of cold-formed steel channel sections with web holes subjected to interior-one-flange loading condition-Part I: Experimental and numerical investigation, *Thin Walled Struct.*, **111** (2017), 103−112. doi: 10.1016/j.tws.2016.10.024.
34. Y. Lian, A. Uzzaman, J. B. Lim, G. Abdelal, D. Nash, B. Young, Web crippling behaviour of cold-formed steel channel sections with web holes subjected to interior-one-flange loading condition-Part II: parametric study and proposed design equations, *Thin Walled Struct.*, **114** (2017), 92−106. doi: 10.1016/j.tws.2016.10.018.
35. C. H. Pham, Shear buckling of plates and thin-walled channel sections with holes, *J. Constr. Steel Res.*,**128** (2017), 800−811. doi: 10.1016/j.jcsr.2016.10.013.
36. P. Keerthan, M. Mahendran, Improved shear design rules for lipped channel beams with web openings, *J. Constr. Steel Res.*, **97** (2014), 127−142. doi: 10.1016/j.jcsr.2014.01.011.
37. B. Chen, K. Roy, A. Uzzaman, G. Raftery, J. B. P. Lim, Parametric study and simplified design equations for cold-formed steel channels with edge-stiffened holes under axial compression, *J. Constr. Steel Res.*, **144** (2020), 106161. doi: 10.1016/j.jcsr.2020.106161.
38. B. Chen, K. Roy, A. Uzzaman, G. Raftery, J. B. P. Lim, Axial strength of back-to-back cold-formed steel channels with edge-stiffened holes, un-stiffened holes and plain webs, *J. Constr. Steel Res.*, **174** (2020), 106313. doi: 10.1016/j.jcsr.2020.106313.
39. A. Uzzaman, J. B. P. Lim, D. Nash, K. Roy, Web crippling behaviour of cold-formed steel channel sections with edge-stiffened and unstiffened circular holes under interior-two-flange loading condition, *Thin Walled Struct.*, **154** (2020), 106813. doi: 10.1016/j.tws.2020.106813.
40. A. Uzzaman, J. B. P. Lim, D. Nash, K. Roy, Cold-formed steel channel sections under end-two-flange loading condition: Design for edge-stiffened holes, unstiffened holes and plain webs, *Thin Walled Struct.*, **147** (2020), 106532. doi: 10.1016/j.tws.2019.106532.
41. B. Chen, K. Roy, A. Uzzaman, J. B. P. Lim, Moment capacity of cold-formed channel beams with edge-stiffened web holes, un-stiffened web holes and plain webs, *Thin Walled Struct.*, **157** (2020), 107070. doi: 10.1016/j.tws.2020.107070.

42. ABAQUS, *ABAQUS/Standard user's manual volumes I-III and ABAQUS CAE manual*, Dassault Systemes Simulia Corporation, (2014). Available from: https://xueshu.baidu.com/usercenter/paper/show?paperid=7918111e014ff6f8228180441bbaeead.
43. X. Yao, *The buckling and interactive buckling behavior and design method of cold-formed steel lipped channel section with holes*, Postdoctoral Report, Nanchang Institute of Technology, (2018).